Int J Thermophys (2007) 28:1245–1254
DOI 10.1007/s10765-007-0237-4

# Liquid–Liquid Coexistence Curve of *n*-Perfluorohexane–*n*-Hexane System

**R. A. Khairulin · S. V. Stankus · V. A. Gruzdev**

Received: 14 November 2006 / Accepted: 22 July 2007 / Published online: 3 September 2007

**Abstract** The shape of the liquid–liquid phase boundary of the $C_6F_{14}$–$C_6H_{14}$ system near the critical solution point has been determined by a $\gamma$-ray attenuation technique. According to the measurements, the critical solution temperature and composition are $295.69 \pm 0.02$ K and $36.1 \pm 0.3$ mol% $C_6F_{14}$, respectively. The critical exponent of the liquid–liquid coexistence curve is $0.322 \pm 0.008$. Midpoints of the coexistence curve exhibit a departure from the law of the rectilinear diameter.

**Keywords** Critical exponent · Critical point · Hexane · Liquid–liquid equilibria · Perfluorohexane

## 1 Introduction

Binary liquid systems of alkanes and perfluoroalkanes have large regions of liquid–liquid immiscibility. The critical solution point of *n*-perfluorohexane–*n*-hexane mixtures is close to room temperature; thus, they are suitable candidates for study and, in particular, for testing of theoretical predictions concerning the behavior of matter in the critical region. Nevertheless, the behavior of the liquid–liquid coexistence curve near the critical point has not been sufficiently explored, and literature data are somewhat contradictory [1,2]. In this article are presented new data for the liquid–liquid phase boundary of the $C_6F_{14}$–$C_6H_{14}$ system, obtained by the $\gamma$-ray attenuation technique. The authors previously used this method to explore a number of binary liquid metal systems with a miscibility gap [3,4], and these measurements established its reliability.

---

R. A. Khairulin (✉) · S. V. Stankus · V. A. Gruzdev
Institute of Thermophysics, Siberian Branch of the Russian Academy of Sciences, Lavrentyev Ave. 1,
Novosibirsk 630090, Russia
e-mail: gamma@itp.nsc.ru

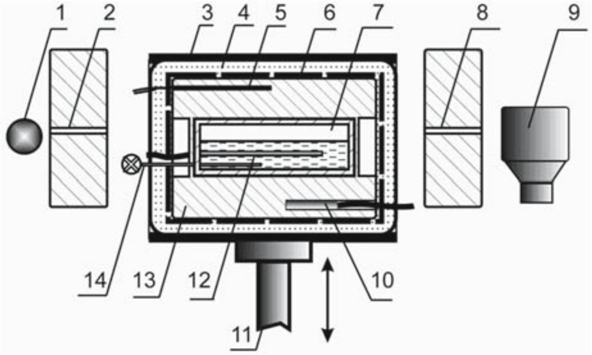

**Fig. 1** Basic schematic of the gamma-densimeter: (1) gamma ray source ($^{137}$Cs); (2, 8) collimators; (3) body; (4) heat-insulating layer; (5) thermocouple; (6) heater; (7) cell; (9) scintillation counter; (10, 12) Pt resistance thermometers; (11) lifting gear; (13) thermostating block (duralumin); (14) tube with valve

## 2 Experimental

The measurements were carried out using a P-2M $\gamma$-densimeter of the Institute of Thermophysics SB RAS [5], equipped with a new measurement cell, which was specially designed for these experiments (Fig. 1). For the $\gamma$-ray source, we use $^{137}$Cs isotope having an activity of 50 GBq and a photon energy of 662 keV. The narrow beam of gamma quanta penetrates through the cell containing the two-phase system. The intensity of the transmitted radiation is measured with a scintillation counter. The experimental cell is a thick-walled titanium cylinder, 30 mm in internal diameter and 115 mm in length. The face planes of the cylinder are closed with titanium caps. The volume is connected with a filling vessel, liquid level regulation system, and vacuum pump by means of an arrangement of valves. The cell is placed in a dry thermostat. The temperature in the thermostat is held to within ±3 mK throughout the measurements. The lifting gear allows for vertical movement of the installation with respect to the beam. This makes it possible for concurrent measurements of the $\gamma$-ray attenuation coefficient in both phases in equilibrium. The temperature of the samples is measured on ITS-90 with a 50 Ω platinum resistance thermometer calibrated at the Siberian Scientific Research Institute of Metrology, Novosibirsk. The uncertainty of the temperature in the range from 283 to 303 K does not exceed ±0.02 K, including the error of the calibration and the temperature gradients. The relative temperature in this interval was accurate to better than ±5 mK.

The law of radiation attenuation in a binary mixture with components $A$ and $B$ may be written as [3,4]

$$\frac{S_A X + S_B(1-X)}{V(X)} = \frac{1}{l}\ln\left[\frac{J_0}{J}\right], \tag{1}$$

where $J$ and $J_0$ are the intensities of the radiation after passage through the cell with and without the sample, respectively; $l$ is the attenuation length; $X$ and $V(X)$ are the molar concentration of component $A$ and the molar volume of the mixture at the site of the beam passage; and $S_i (i = A, B)$ are attenuation sections of the components.

With a knowledge of the concentration dependence of the molar volume, $V(X)$, Eq. 1 enables determination of the concentration at the site of the beam passage. By moving the cell in a vertical direction and measuring the $\gamma$-ray attenuation above and below the two-liquid interface, we can measure the compositions of the coexisting phases in the liquid system with a miscibility gap. If the mean composition of the mixture is close to the critical concentration, the shape of the coexistence curve may be reconstructed by measurements of the temperature dependences of the $\gamma$-ray attenuation coefficients in the two phases, using only a single sample. We investigated the specimen containing 35.04 mol% $C_6F_{14}$. This composition was found to be very close to the critical concentration (see below).

## 3 Results and Discussion

### 3.1 Density of the Constituents and the Homogeneous Solution

As noted above, data on the concentration dependence of the molar volume $V(X)$ are needed to determine the compositions of the phases of the separated mixture. For this purpose we investigated the temperature dependences of the density of $n$-perfluorohexane and $n$-hexane. The $n$-hexane sample was supplied by the Novosibirsk Institute of Organic Chemistry SB RAS with a stated minimum purity of 99.6 mol%. It was used without further purification. $n$-Perfluorohexane (Fluorochem, 99 mass%) was boiled for the purpose of removing dissolved gases and volatile components. The density of the liquids at room temperature and atmospheric pressure was measured by the indirect Archimedean method to within an uncertainty of less than 0.03%. Then, using these reference data, we determined the temperature dependences of the component densities by the relative version of the $\gamma$-ray attenuation method [5] in the range from 293 to 350 K. Our data for the density are presented in Figs. 2 and 3. The density of liquid $n$-hexane was measured along the saturation line. Liquid $n$-perfluorohexane in the first test also was in equilibrium with its vapor. But in the second experiment the cell was not preliminarily evacuated, so the gaseous phase above the liquid (about 15% of the cell volume) was a mixture of air and $C_6F_{14}$ vapor. The results of these two measurements agree, to within the estimated uncertainty (0.1–0.15%). That is, a possible dissolving of $O_2$ and $N_2$ in liquid $n$-perfluorohexane has no marked effect on its density in the temperature interval under study. Our data coincide with most available literature results, to within combined errors. The results of the experiments with pure $C_6F_{14}$ and $C_6H_{14}$ were also used for defining the $\gamma$-ray attenuation sections of the components.

The mixture specimen containing 35.04 mol% $C_6F_{14}$ was prepared using an analytical balance with a precision of ±0.3 mg. Corrections were made to account for the evaporation of constituents in the mixing vessel (for these evaluations we used information about vapor–liquid equilibria for $n$-perfluorohexane, $n$-hexane, and their mixtures from the NIST Chemistry Web Book [9] and [2]). The specimen volume was about 65 $cm^3$. Before filling the experimental cell, the mixture was heated above the

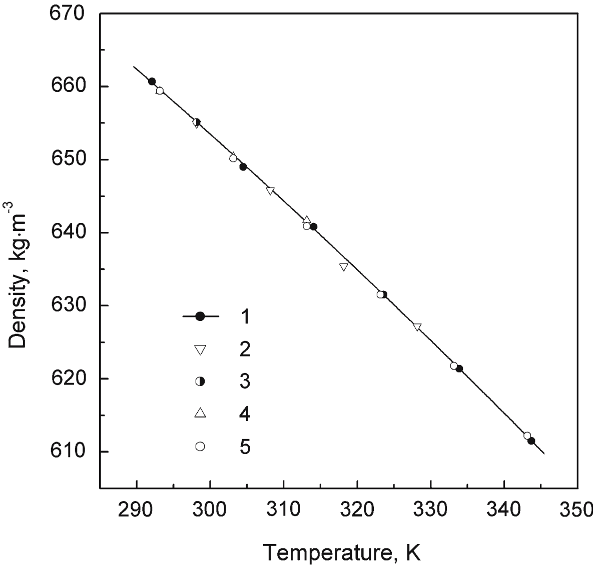

**Fig. 2** Density of *n*-hexane as a function of temperature: (1) Present work; (2) Bedford and Dunlap [1]; (3) Lepori et al. [6]; (4) Landolt-Börnstein [7]; (5) Rossini et al. [8]

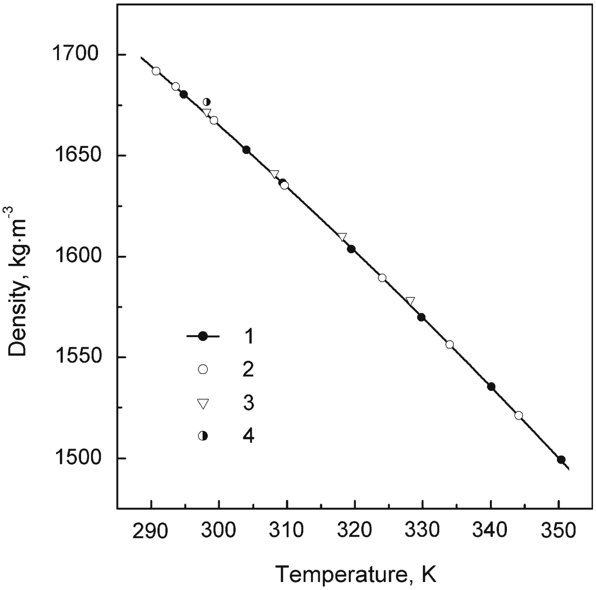

**Fig. 3** Density of *n*-perfluorohexane as a function of temperature: (1, 2) Present work (experiments 1 and 2, respectively); (3) Bedford and Dunlap [1]; (4) Lepori et al. [6]

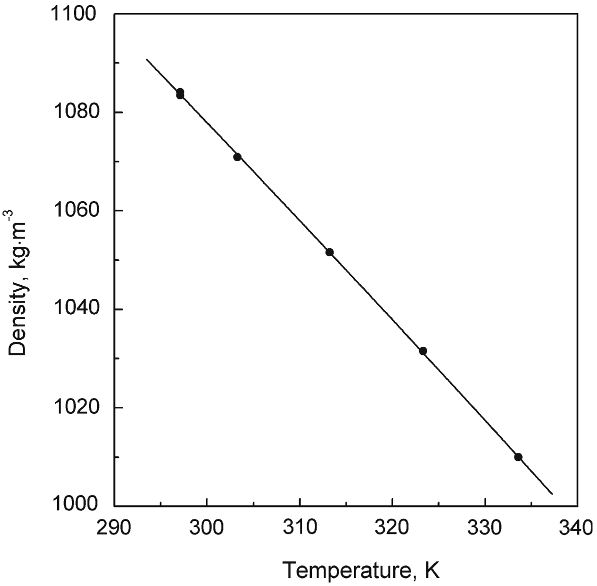

**Fig. 4** Temperature dependence of the density of *n*-perfluorohexane–*n*-hexane solution at 35.04 mol% $C_6F_{14}$ (data of this work)

critical solution temperature (up to 298 K) and was thoroughly mixed. During filling, the cell and connecting tube also were heated to about 298 K; thus, the solution remained homogeneous, and a small loss of material did not change the concentration. The liquid phase occupied about 80% of the cell volume. According to our estimates, variations of the mean composition of the liquid mixture connected with the difference in volatilities of the components did not exceed 0.03 mol% in the temperature range under study.

At a first stage in our experiments with the mixture, we determined its density in the homogeneous region. The sample was heated well above the critical temperature (up to 330 K) and was stirred thoroughly by shaking of the installation. The solution homogeneity was checked by measuring the $\gamma$-ray attenuation coefficients at different heights. The temperature dependence of the density of the homogeneous mixture was measured using the absolute version of the $\gamma$-ray attenuation method [5] in the range from 297 to 333 K (Fig. 4).

The data for the densities of the constituents and the solution containing $X_M = 0.3504$ mole fraction of $C_6F_{14}$ (35.04 mol% $C_6F_{14}$) were used to define the concentration and temperature dependence of the molar volume $V(X, T)$ of the *n*-perfluorohexane–*n*-hexane system. For most liquid binary systems with a miscibility gap, the $X$-dependence of the excess mixing volume $V_E(X)$ is close to a parabola with an extreme at 0.5 mole fraction (or 50 mol%). In this connection, we used the following relation for the construction of $V(X, T)$:

$$V(X, T) = V_{C_6F_{14}}(T)X + V_{C_6H_{14}}(T)(1 - X) + V_E(X_M, T)\frac{X(1 - X)}{X_M(1 - X_M)}, \quad (2)$$

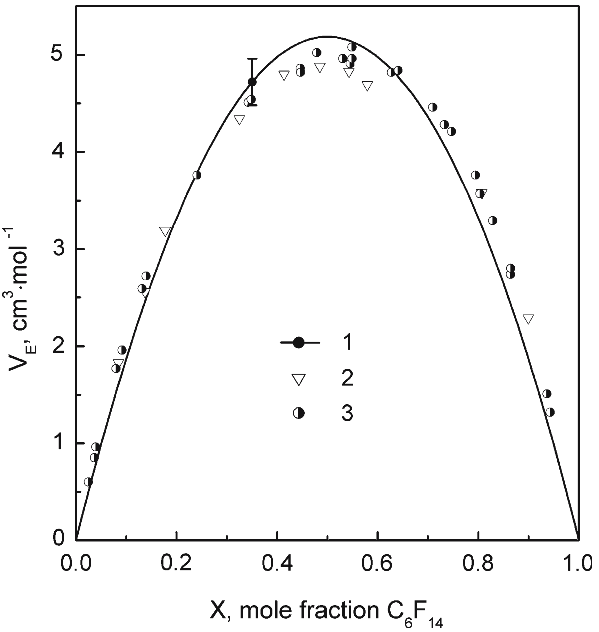

**Fig. 5** Concentration dependence of excess molar volume for $n$-perfluorohexane–$n$-hexane system at 298.15 K. (1) Present work, experimental value for $X_M$ = 0.3504 mole fraction of $C_6F_{14}$ and $V_E(X)$ calculated by Eq. 2; (2) Bedford and Dunlap [1]; (3) Lepori et al. [6]

As seen from Fig. 5, the experimental data for excess molar volumes of $n$-perfluorohexane–$n$-hexane mixtures are in good agreement with $V_E$ values calculated by Eq. 2. It should be noted that the errors in molar volume connected with the approximate nature of Eq. 2 do not produce a marked effect on the accuracy of the determination of the local concentration of the separated mixture if the latter is not too different from the mean composition $X_M$. According to our evaluations [10], the error $\Delta X$ does not exceed 0.1–0.15 mol% when $|X - X_M| \leq$ 15–20 mol%.

### 3.2 Liquid–Liquid Equilibria

The investigation of liquid–liquid equilibria was conducted in the following way. Starting at 296 K, the homogeneous specimen containing 35.04 mol% $C_6F_{14}$ was cooled at a rate of no more than 0.1 K · h$^{-1}$. The onset of the phase separation was determined from a dramatic change of the intensity of the radiation passed through the sample. Thereafter, the cooling was stopped, and the height dependence of the radiation intensity was determined in order to locate the two-liquid interface. It should be noted that the sample scanning near the critical mixing point did not detect a gravity effect, which was observed in the fluids near the gas–liquid critical point [5]. Within the limits of random error, the density and the distribution of the components in both layers was independent of the height. The measurements of the temperature dependences of the $\gamma$-ray attenuation coefficients above and below the interface were conducted during step-by-step cooling. After each step, the specimen was held sufficiently long at constant temperature to establish equilibrium. We believed that equilibrium was reached, if a variation of the intensity of transmitted radiation for a time 20–25 min was no larger than the statistical error.

The data for the liquid–liquid phase boundary as determined from the measurements and Eqs. 1 and 2 are presented in Table 1 and Fig. 6. A comparison with literature results reveals that our data are in excellent agreement with the results of Bedford and Dunlap [1]. Unfortunately, there are only a few experimental points in Ref. [1], especially in the immediate vicinity of the critical point.

**Table 1** Experimental data on the compositions and molar volumes of the phases along the liquid–liquid coexistence curve of *n*-perfluorohexane–*n*-hexane system

| $C_6F_{14}$-rich phase | | | $C_6H_{14}$-rich phase | | |
|---|---|---|---|---|---|
| $T$(K) | $X$(mol% $C_6F_{14}$) | $V$ ($\mathrm{cm^3 \cdot mol^{-1}}$) | $T$(K) | $X$ (mol% $C_6F_{14}$) | $V$ ($\mathrm{cm^3 \cdot mol^{-1}}$) |
| 295.674 | 39.88 | 164.2 | 295.674 | 32.32 | 158.4 |
| 295.622 | 41.97 | 165.7 | 295.622 | 30.33 | 156.9 |
| 295.519 | 43.97 | 167.2 | 295.519 | 28.69 | 155.5 |
| 295.218 | 47.11 | 169.3 | 295.218 | 25.77 | 153.1 |
| 294.809 | 50.02 | 171.3 | 294.810 | 23.61 | 151.3 |
| 294.204 | 52.54 | 172.8 | 294.204 | 21.38 | 149.3 |
| 293.206 | 56.23 | 175.0 | 293.207 | 19.01 | 147.1 |
| 292.059 | 59.21 | 176.6 | 292.057 | 17.04 | 145.2 |
| 290.965 | 61.38 | 177.7 | 290.966 | 15.63 | 143.8 |
| 289.419 | 64.05 | 178.9 | 289.417 | 14.03 | 142.1 |

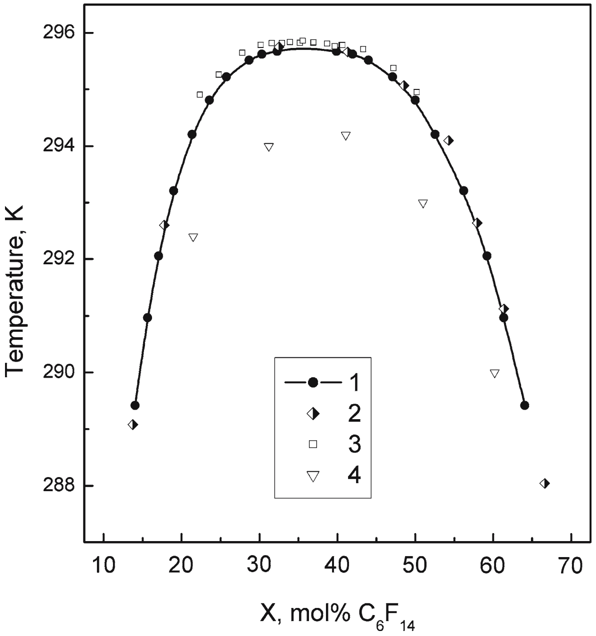

**Fig. 6** Liquid–liquid phase boundary for *n*-perfluorohexane–*n*-hexane system. (1) Present work; (2) Bedford and Dunlap [1]; (3) Gaw and Scott [11]; (4) Duce et al. [2]

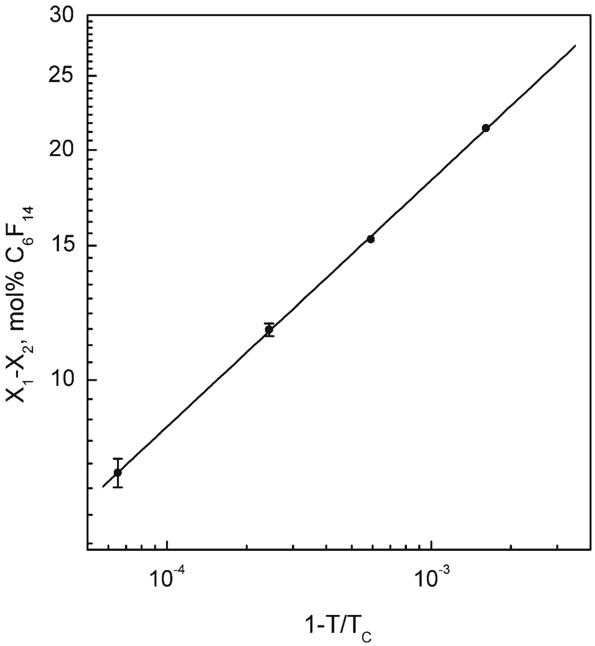

**Fig. 7** Difference of compositions of the coexisting phases versus relative temperature (in log coordinates) along the liquid–liquid equilibrium line of *n*-perfluorohexane–*n*-hexane system. Circles are experimental points. Straight line is best fit of the experimental data by Eq. 3

According to a recent view on the nature of critical phenomena, the binary liquids near the critical mixing point and the fluids near the gas–liquid critical point obey the universal scaling laws [12]. For binary liquids, the molar concentration $X$ is the order parameter, analogous to the magnetization of idealized three-dimensional Ising magnetic and the density of fluid [13]. The asymptotic behavior of the liquid–liquid coexistence curve in the vicinity of the critical point is described by the following power law [12]:

$$(X_1 - X_2) = A\varepsilon^{\beta}. \tag{3}$$

Here, $X_1$, $X_2$ are molar concentrations of the phases in equilibrium with each other, $\varepsilon = 1 - T/T_C$, $T_C$ is the critical temperature, $A$ is a constant, and $\beta$ is the critical exponent of the coexistence curve. To determine the critical exponent and critical temperature, data from Table 1 over the range of $\varepsilon$ from $6.5 \times 10^{-5}$ to $1.6 \times 10^{-3}$ (at higher $\varepsilon$, the asymptotic relation ceases to hold) were fitted with Eq. 3 which gave $A = 168.9 \pm 9.1$, $T_C = 295.693 \pm 0.02$ K, and $\beta = 0.322 \pm 0.008$ (Fig. 7). In principle, the experimental $\beta$ is close to the theoretical critical index calculated from the Ising model: according to various methods, the calculated value lies in the range from 0.31 to 0.34 [12,14]. But, it is pointed out in the literature that measured critical exponents for liquid–liquid coexistence curves of mixtures (0.31–0.33), on average, are somewhat less than those for liquid–vapor equilibrium lines of pure substances (0.34–0.35) [12]. Our results also confirm the existence of the above-mentioned contradiction with scaling theory, which suggests universality of the critical indexes.

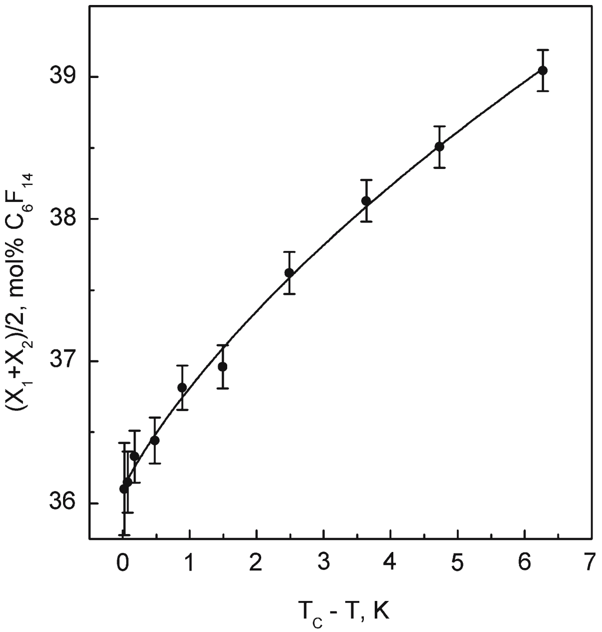

**Fig. 8** Midpoints of the liquid–liquid coexistence curve of *n*-perfluorohexane–*n*-hexane system versus relative temperature. Points are experimental data. Line is best fit by Eq. 4

The midpoints of the two-liquid phase boundary $\overline{X} = (X_1 + X_2)/2$ exhibit deviations from the classical law of the rectilinear diameter near the critical temperature; see Fig. 8. This feature of the diameter is predicted by scaling theory, according to which [15] the temperature dependence of $\overline{X}$ in the vicinity of the critical point is described by the relationship,

$$\overline{X} = X_C + A_1\varepsilon + A_2\varepsilon^{1-\alpha} + A_3\varepsilon^{2\beta}, \tag{4}$$

where $X_C$ is the critical concentration; $\alpha \approx 0.11$ is the critical exponent of heat capacity; and $A_1$, $A_2$, $A_3$ are constants. In our case the deviations from a straight line slightly exceed the measurement errors (the error bars in Figs. 7 and 8 also include the uncertainty in the concentrations connected with the uncertainty of the relative temperature: $\Delta X_{1,2} = (\partial X_{1,2}/\partial\varepsilon)\Delta\varepsilon$; near the critical point, these errors give the main contribution to the total uncertainty, because $[\partial X_{1,2}/\partial\varepsilon] \to \infty$ when $\varepsilon \to 0$). Nevertheless, we used Eq. 4 to approximate the experimental data for the midpoints and to determine the critical composition. The best fit gives $X_C = 36.1 \pm 0.3$ mol% $C_6F_{14}$.

**Acknowledgments** We gratefully acknowledge the financial support for this research from the Siberian Branch of the Russian Academy of Sciences (Grant IG-06-No.81) and the Russian Foundation for Basic Research (Grant No. 05-08-01173).

## References

1. R.G. Bedford, R.D. Dunlap, J. Am. Chem. Soc. **80**, 282 (1958)
2. C. Duce, M.R. Tinè, L. Lepori, E. Matteoli, Fluid Phase Equilib. **199**, 197 (2002)
3. R.A. Khairulin, S.V. Stankus, J. Phase Equilib. **20**, 148 (1999)
4. R.A. Khairulin, S.V. Stankus, A.L. Sorokin, J. Non-Crystalline Solids **297**, 120 (2002)
5. S.V. Stankus, R.A. Khairulin, Int. J. Thermophys. **27**, 1110 (2006)
6. L. Lepori, E. Matteoli, A. Spanedda, C. Duce, M.R. Tinè, Fluid Phase Equilib. **201**, 119 (2002)
7. A. Eucken, K. Hellwege, *Landolt-Börnstein: Zahlenwerte und Funktionen aus Physik, Chemie, Astronomie, Geophysik und Technik* (Springer Verlag, Berlin, 1951)
8. F.D. Rossini, K.S. Pitzer, R.L. Arnett, R.M. Braun, G.C. Pimentel, *Selected Values of Physical and Thermodynamic Properties of Hydrocarbons and Related Compounds* (Carnegie Press, Pittsburgh, 1953)
9. http://webbook.nist.gov/chemistry
10. R.A. Khairulin, S.V. Stankus, P.P. Bezverkhy, J. Alloys Compd. **312**, 211 (2000)
11. W.J. Gaw, R.L. Scott, J. Chem. Thermodyn. **3**, 335 (1971)
12. M.A. Anisimov, *Critical Phenomena in Liquids and Liquid Crystals* (Nauka Pub., Moscow, 1987) [in Russian]
13. J.V. Sengers, J.M.H. Levelt Sengers, *Progress in Liquid Physics* (Wiley, New York, 1978)
14. M.E. Fisher, *The Nature of Critical Points* (University of Colorado Press, Boulder, Colorado, 1965)
15. Y.C. Kim, M.E. Fisher, G. Orkoulas, Phys. Rev. E **67**, 061506 (2003)